

Balancing Control of Two Wheeled Mobile Robot Based on Decoupling Controller

AHMED J. ABOUGARAIR

Electrical and Electronics Engineering Dep
University of Tripoli
Tripoli – LIBYA
a.abougarair@uot.edu.ly

ELFITURI S. ELAHEMER

Mechatronic Systems Engineering Dep.
Simon Fraser University
Vancouver-Canada
elahemer@sfu.ca

Abstract: -Nowadays, Two Wheeled Inverted Pendulum Mobile Robots (TWIPMR) are being used widely in many different applications. It's very important to ensure that the robot is able to stabilize itself when it moves forward and backward. Stabilization and the trajectory tracking of the robot has gained extensive momentum and become increasingly popular with researchers around the world. In addition, the robot must regulate the steering angle when it turns left or right must be considered in control design and analysis beside stability and the trajectory tracking. To achieve these, two decoupling optimal controllers based on Linear Quadratic Regulator (LQR) design method are proposed in this paper to robustly balance the robot platform and to generate the required optimal control signals under any external disturbances. The simulation results are provided to show the effectiveness of the proposed designed control method to get an accurate tracking signal of the desired trajectory. Furthermore, the 3D representation of the simulation and a visualization model to observe robot behavior in different scenarios is included

Key-Words: -TWIPMR - LQR controller - Decoupling Controller - VRML model.

1 Introduction

Design and control of two-wheeled balancing mobile robot or wheeled inverted pendulum is a popular research topics in verifying various control theories over the last decade. The motion control problem of the robot that can autonomously self-balanced on wheels has received much attention in both academic and industry worldwide. Two-wheeled robot system is not only intricate multiple-input multiple-output nonlinear system, but also a kind of typical non-holonomic system with time-varying. It is also a complicated coupled dynamic system and non-linear saturation dynamic characteristics [1],[2]. In real movement, the two-wheeled robot suffers from uncertain factors, such as load change, the friction, road conditions and external interference, this would bring great difficulties to motion control of two- wheeled robot. In this work, the performance of the dynamical system is being controlled till the desired trajectory is optimized. A decoupling controller based on Linear Quadratic Regulator (LQR) is designed and implemented to robustly stabilize the TWIPMR system [3]. In addition, the tracking performance of the robot displacement under the influence of the disturbance is investigated and analyzed. The rest work of the paper is organized as follows. In section 2, the mathematical model of TWIPMR robot is presented in a systematic way and derived .In

section 3, the system input-output analysis is explained. The decoupling controller is designed in section 4. The virtual reality animation for simulation and analysis is shown. Finally, section 5 presented the conclusion.

2 Mathematical Model of TWIPMR

The performance of a balancing robot depends on the efficiency of the control algorithms and the dynamic model of the system. By adopting the coordinate system shown in Fig.1 using Newtonian mechanics, it can be shown that the dynamics of the TWIPMR under this consideration is governed by the following equations of motion. Linear displacement of the vehicle is denoted by x , angular rotation about the y-axis (pitch) by θ , and angular rotation about the z-axis (yaw) by δ [4]. The definitions of parameters are in listed in Table 1.

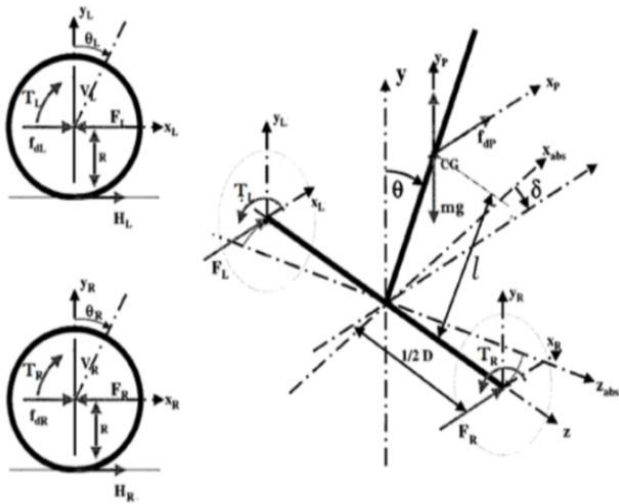


Fig. 1: Diagram of forces and moments acting on the TWIPMR [4]

Table 1: Definition of parameters of the system

Symbol	Definition
m	Mass of robot body
R	Radius of wheel
D	Distance between wheels
f _p	Disturbances applied CG
CG	Center of gravity of robot body
l	Distance between CG and wheel axis.
J _δ	Moment of inertia of chassis with respect to y-axis
J _{mo}	Moment of inertia of chassis
J _{po}	Moment of inertia of pendulum
F _p	Horizontal force
T _L , T _R	Torques generated from the motors
θ _L , θ _R	Rotation angles of wheels
H _L , H _R	Friction forces with ground surface
F _{dL} , F _{dR}	Outside Disturbances applied to wheels
F _L , F _R	Interacting forces between wheels and chassis
J _L , J _R	Moment of inertia of wheels with respect to z-axis
M _L , M _R	Mass of each wheel

A mechanical 3 DOF system can be modeled using six state space variables. The following variable has been chosen:

- x: Straight line position [m]
- v: Straight line speed [m/s]
- θ: Pitch angle [rad]
- ω: Pitch rate [rad/s]
- δ: Yaw angle [rad]
- δ̇: Yaw rate [rad/s]

Based on these parameters the state space equation for the system is obtained as [5]:

$$\dot{x} = v \tag{1}$$

$$\dot{v} = \frac{T_R}{\alpha R} + \frac{F_{dL}}{\alpha} + \frac{F_{dR}}{\alpha} + \frac{f_p T_R}{\alpha \alpha R} + \frac{F_{dL}}{\alpha} + \frac{F_{dR}}{\alpha} + \frac{f_p}{\alpha} - \frac{m l \cos \theta}{\alpha (J_{mo} + J_{po})} \left[\frac{m g l \sin \theta + f_p l \cos \theta}{\alpha} \right] \tag{2}$$

$$\dot{\theta} = \omega \tag{3}$$

$$\dot{\omega} = \frac{(m g l \sin \theta + f_p l \cos \theta) (M + m + 4M_w + \frac{2J_w}{R^2}) + \beta}{\beta} + \frac{m l \cos \theta (\frac{T_L}{R} + \frac{T_R}{R} + F_{dL} + F_{dR} + f_p)}{\beta} \tag{4}$$

$$\dot{\delta} = \Omega \tag{5}$$

$$\dot{\Omega} = \frac{D}{2} \left[\frac{\frac{T_L}{R} - \frac{T_R}{R} + F_{dL} - F_{dR}}{J_{\delta} + \frac{D^2}{2} [\frac{J_w}{R^2} + M_w]} \right] \tag{6}$$

With α and β are defined as following

$$\alpha = M + m + 4M_w + \frac{2J_w}{R^2} + \left[\frac{m^2 l^2 \cos^2 \theta}{(J_{mo} + J_{po})} \right]$$

$$\beta = (J_{mo} + J_{po}) \left(M + m + 4M_w + \frac{2J_w}{R^2} \right) + m^2 l^2 \cos^2 \theta$$

The nonlinear dynamic equations represented using simulink model as shown in Fig. 2. It gives the exact relationships among all the variables involved. Due to small variation about operating conditions at θ = 0, the above equations are linearized and the following linear model equations are obtained [5].



Fig. 2: Simulink model of the nonlinear TWIPMR dynamics system

$$\dot{x} = v \tag{7}$$

$$\dot{v} = \frac{T_L}{\alpha R} + \frac{T_R}{\alpha R} + \frac{F_{dL}}{\alpha} + \frac{F_{dR}}{\alpha} + \frac{(J_{mo}+J_{po})-ml^2}{\alpha(J_{mo}+J_{po})} f_p - \frac{m^2 g l^2}{\alpha(J_{mo}+J_{po})} \theta \tag{8}$$

$$\dot{\theta} = \omega \tag{9}$$

$$\dot{\omega} = \frac{\left(\frac{mlT_L}{R} + \frac{mlT_R}{R} + mlF_{dL} + mlF_{dR}\right) + (mg l \theta + f_p l)}{\beta} + \frac{\left(M+m+4M_w + \frac{2J_w}{R^2}\right) + ml f_p}{\beta} \tag{10}$$

$$\dot{\delta} = \Omega \tag{11}$$

$$\dot{\Omega} = \frac{D}{2} \left[\frac{\frac{T_L}{R} - \frac{T_R}{R} + F_{dL} - F_{dR}}{J_{\delta} + \frac{D^2}{2} \left(\frac{J_w}{R^2} + M_w\right)} \right] \tag{12}$$

Where

$$\alpha = M + m + 4M_w + \frac{2J_w}{R^2} + \left[\frac{m^2 l^2}{(J_{mo} + J_{po})} \right]$$

$$\beta = (J_{mo} + J_{po}) \left(M + m + 4M_w + \frac{2J_w}{R^2} \right) + m^2 l^2$$

The general state-space representation of a continuous LTI system can be written in the following form:

$$\begin{bmatrix} \dot{x} \\ \dot{v} \\ \dot{\theta} \\ \dot{\omega} \\ \dot{\delta} \\ \dot{\delta} \end{bmatrix} = \begin{bmatrix} 0 & 1 & 0 & 0 & 0 & 0 \\ 0 & 0 & A_{23} & 0 & 0 & 0 \\ 0 & 0 & 0 & 1 & 0 & 0 \\ 0 & 0 & A_{43} & 0 & 0 & 0 \\ 0 & 0 & 0 & 0 & 0 & 1 \\ 0 & 0 & 0 & 0 & 0 & 0 \end{bmatrix} \begin{bmatrix} x \\ v \\ \theta \\ \omega \\ \delta \\ \dot{\delta} \end{bmatrix} + \begin{bmatrix} 0 \\ B_{21} & B_{22} & B_{23} & B_{24} & B_{25} \\ 0 & 0 & 0 & 0 & 0 \\ B_{41} & B_{42} & B_{43} & B_{44} & B_{45} \\ 0 & 0 & 0 & 0 & 0 \\ B_{61} & B_{62} & B_{63} & B_{64} & 0 \end{bmatrix} \begin{bmatrix} T_L \\ T_R \\ F_{dL} \\ F_{dR} \\ f_p \end{bmatrix} \tag{13}$$

Where

$$A_{23} = -\frac{m^2 g l^2}{\alpha(J_{mo}+J_{po})}, \quad A_{43} = \frac{(M+m+4M_w + \frac{2J_w}{R^2})mgl}{\beta}$$

$$B_{21} = B_{22} = \frac{1}{R\alpha}, \quad B_{23} = B_{24} = \frac{1}{\alpha}$$

$$B_{25} = \frac{(J_{mo}+J_{po})-ml^2}{\alpha(J_{mo}+J_{po})}, \quad B_{41} = B_{42} = \frac{ml}{R\beta}$$

$$B_{43} = B_{44} = \frac{ml}{\beta}, \quad B_{45} = \frac{(M+m+4M_w + \frac{2J_w}{R^2})l + ml}{\beta}$$

$$B_{61} = \frac{D}{2R} \left[\frac{1}{J_{\delta} + \frac{D^2}{2} \left(\frac{J_w}{R^2} + M_w\right)} \right], \quad B_{62} = -B_{61}$$

$$B_{63} = \frac{D}{2} \left[\frac{1}{J_{\delta} + \frac{D^2}{2} \left(\frac{J_w}{R^2} + M_w\right)} \right], \quad B_{64} = -B_{63}$$

3 System Analysis

The TWIPMR system can be defined as a MIMO system where $(T_L, T_R, F_{dL}, F_{dR}, f_p)$ the inputs are and $(x, \dot{x}, \theta, \dot{\theta}, \delta, \dot{\delta})$ are the outputs states. The system transfer functions are summarized in table 2. The transfer functions have at least one or more unstable poles. The open loop step and impulse responses are shown in Fig 3. It can be clearly seen that all responses are diverging and the system is unstable. Also a rapid divergence in the output is observed when a little variations in the input signal is occurred. [6],[7]. Consequently, in order to avoid this degradation in stability and tracking performance, the decoupling optimal controller is designed as will be explained in the next section.

Table 2: Transfer Function Matrix

	TL	TR	F _{dR}	F _{dL}	f _p
x	$\frac{1.3 s^2 - 15}{s^4 - 11.2s^2}$	$\frac{1.3 s^2 - 15}{s^4 - 11.2s^2}$	$\frac{0.2 s^2 - 2}{s^4 - 11.2s^2}$	$\frac{0.2 s^2 - 2}{s^4 - 11.2s}$	$\frac{0.2 s^2 - 2}{s^4 - 11.2s}$
\dot{x}	$\frac{1.3 s^2 - 15}{s^3 - 11.2s}$	$\frac{1.3 s^2 - 15}{s^3 - 11.2s}$	$\frac{0.2 s^2 - 2}{s^3 - 11.2s}$	$\frac{0.2 s^2 - 2}{s^3 - 11.2s}$	$\frac{0.2 s^2 - 2}{s^3 - 11.2s}$
θ	$\frac{1.58}{s^2 - 11.2}$	$\frac{1.58}{s^2 - 11.2}$	$\frac{0.27}{s^2 - 11.2}$	$\frac{0.27}{s^2 - 11.2}$	$\frac{1.03}{s^2 - 11.2}$
$\dot{\theta}$	$\frac{1.58 s}{s^2 - 11.2}$	$\frac{1.58 s}{s^2 - 11.2}$	$\frac{0.27 s}{s^2 - 11.2}$	$\frac{0.27 s}{s^2 - 11.2}$	$\frac{1.03s}{s^2 - 11.2}$
δ	$\frac{18.85}{s^2}$	$-\frac{18.85}{s^2}$	$\frac{3.2}{s^2}$	$-\frac{3.2}{s^2}$	0
$\dot{\delta}$	$\frac{18.85}{s}$	$-\frac{18.85}{s}$	$\frac{3.2}{s}$	$-\frac{3.2}{s}$	0

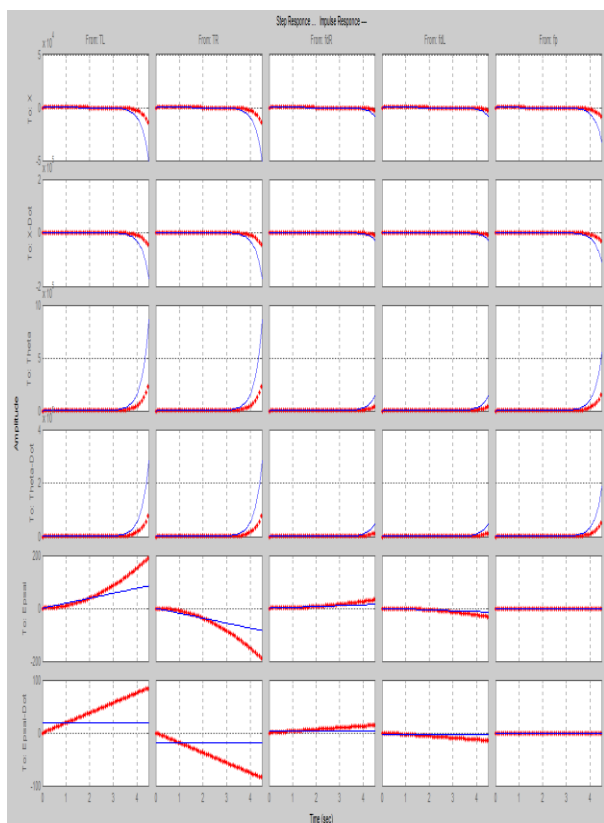


Fig. 3: Open loop unit step and impulse responses of the transfer matrix

4. Decoupling Controller Design

To stabilize the robot, a decoupling methodology using two decoupled state space controllers based on LQR is implemented. In this case, the system equations are decoupled into couple of sets. The first set of equations represents the displacement and the rotational angle about y-axis while the second set represents the rotational angle about z-axis, and accordingly the following model is obtained.

$$\begin{bmatrix} \dot{x} \\ \dot{v} \\ \dot{\theta} \\ \dot{\omega} \end{bmatrix} = \begin{bmatrix} 0 & 1 & 0 & 0 \\ 0 & 0 & A_{23} & 0 \\ 0 & 0 & 0 & 1 \\ 0 & 0 & A_{43} & 0 \end{bmatrix} \begin{bmatrix} x \\ v \\ \theta \\ \omega \end{bmatrix} + \begin{bmatrix} 0 & 0 \\ B_{21} & B_{22} \\ 0 & 0 \\ B_{41} & B_{42} \end{bmatrix} \begin{bmatrix} T_L \\ T_R \end{bmatrix} \quad (14)$$

$$\begin{bmatrix} \dot{\delta} \\ \dot{\delta} \end{bmatrix} = \begin{bmatrix} 0 & 1 \\ 0 & 0 \end{bmatrix} \begin{bmatrix} \delta \\ \delta \end{bmatrix} + \begin{bmatrix} 0 & 0 \\ B_{61} & B_{62} \end{bmatrix} \begin{bmatrix} T_L \\ T_R \end{bmatrix} \quad (15)$$

In order to impose the desired dynamics on the system, the rotation around the z-axis is controlled independently of the rotation around the y-axis. Where two separate LQR controllers are developed. The decoupling controller generates the control signals T_θ and T_δ which are in turn coupled to obtain the correcting control signals T_L and T_R . Fig. 4 shows the closed loop system with decoupling controller. The system can be now represented into

two independent subsystems. As a result, an alternative state space model is obtained [8-10].

$$\begin{bmatrix} \dot{x} \\ \dot{v} \\ \dot{\theta} \\ \dot{\omega} \end{bmatrix} = \begin{bmatrix} 0 & 1 & 0 & 0 \\ 0 & 0 & A_{23} & 0 \\ 0 & 0 & 0 & 1 \\ 0 & 0 & A_{43} & 0 \end{bmatrix} \begin{bmatrix} x \\ v \\ \theta \\ \omega \end{bmatrix} + \begin{bmatrix} 0 \\ B_{21} \\ 0 \\ B_{41} \end{bmatrix} [T_\theta] \quad (16)$$

$$\begin{bmatrix} \dot{\delta} \\ \dot{\delta} \end{bmatrix} = \begin{bmatrix} 0 & 1 \\ 0 & 0 \end{bmatrix} \begin{bmatrix} \delta \\ \delta \end{bmatrix} + \begin{bmatrix} 0 \\ B_{61} \end{bmatrix} [T_\delta] \quad (17)$$

Since this section will only analyses the performance of the decoupled linear quadratic regulation with integral control (LQRIC) and linear quadratic regulation with feedforward scaling factor (LQRFSF) control scheme, two separate LQR controllers need to be designed and tuned, the weighting matrices (Q_θ, Q_δ) and (R_θ, R_δ) were tuned using Bryson's rule until simulation results display the desired system performance. The following is the algorithm that has been used in the LQRFSF and LQRIC control design for TWIPMR system.

Algorithm

- 1- For position-balancing subsystem, using Bryson's rule chose $Q_\theta = \text{diag}(q_1, q_2, q_3, q_4)$ as the matrix A_θ 4x4, where q_1 corresponds to weight on robot position, q_2 corresponds to weight on robot linear velocity, q_3 corresponds to the pitch angle, q_4 corresponds to the angular velocity. Chose $Q_\delta = \text{diag}(q_5, q_6, q_7)$ as the matrix A_δ 3x3, where q_5 corresponds to weight on yaw angle, q_6 corresponds to weight on derivative of yaw angle and q_7 corresponds to weight of integral state.
- 2- Since, the constraint on robot position is difficult to meet, we choose $q_1 \gg q_i, i = 2,3,4,5,6,7$. As the robot begins to fall the linear velocity of the robot should change rapidly to prevent this, so $q_2 \gg q_4$.
3. Due to the physical constraint s imposed on the angle and position we chose $q_1 \gg q_2, q_3 \gg q_4$. As there is constraint we choose R_δ and $R_\theta \ll 1$.

The decoupling controller transform the LQRFSF and LQRIC output signals into torque commands for the left and right motors (T_L, T_R). The motor torque commands are fed into the ATWIPMR plant model, a new set of state variables are produced, and the decoupled control scheme repeats. In other words, the decoupling controller can control the rotation around the z-axis independently of the rotation around the y-axis. The Simulink block diagram of the decoupling unit can be seen in Figure 4.

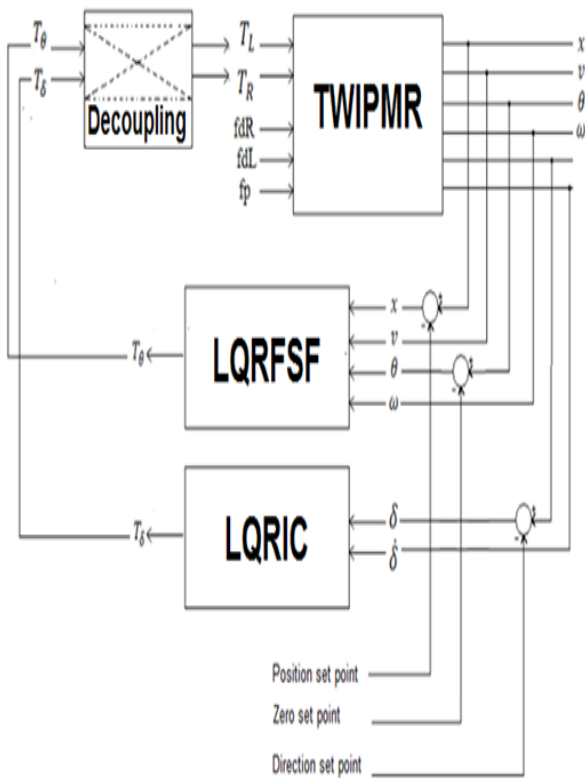


Fig. 4: Control block diagram for the TWIPMR system Decoupling Controller

5. Virtual Reality Animation

The link between the TWIPMR system and the virtual reality model is done through the virtual reality toolbox. In this section the performance of the decoupled LQR control scheme is analyzed. A visualization model is created to make it easier to observe and actually see how the robot behaves in different scenarios. Previously, the user can view the results in 2D after the simulation is complete, by including a virtual world of a TWIPMR system the simulation in 3D animation during the simulation run time [6]. The virtual model is created using the standard Virtual Reality Modeling Language (VRML). It is a text language used for describes 3-D shapes and interactive environments. Design in VRML depends on the information available to the designer and the imaging of the object. The VRML model of TWIPMR is processed using the V-Realm Builder as shown in Fig. 5.

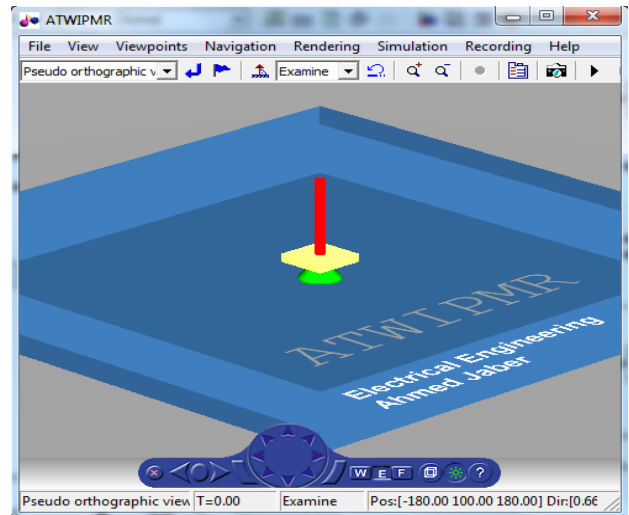


Fig. 5: VRML model of the ATWIPMR in V-Realm

The link between Matlab-Simulink and VR environment is used for the manipulator’s movements. The visualization is implemented in simulink as a separate part as shown in Fig. 6. Inputs to the VR Sink block are the signals that are necessary to calculate position and rotation of the objects in the VRML model.

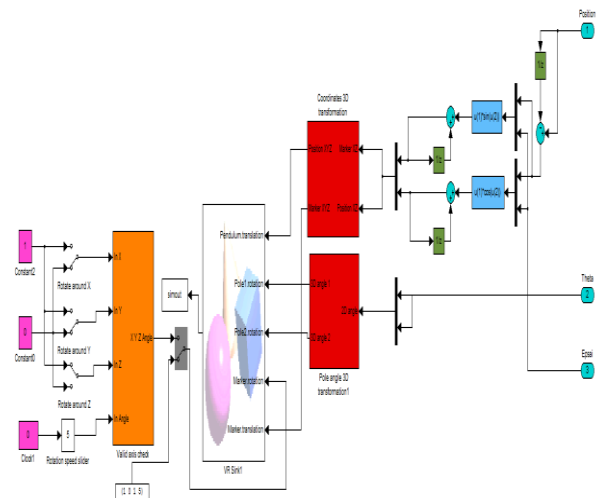


Fig. 6: Virtual Reality World Interface

Fig. 7 shows a complete simulink model for testing the controller. Every part of the system is implemented in a simulink model as a separate block. The effects of disturbances (F_{dL} , F_{dR} , f_p) are investigated and taken into consideration.

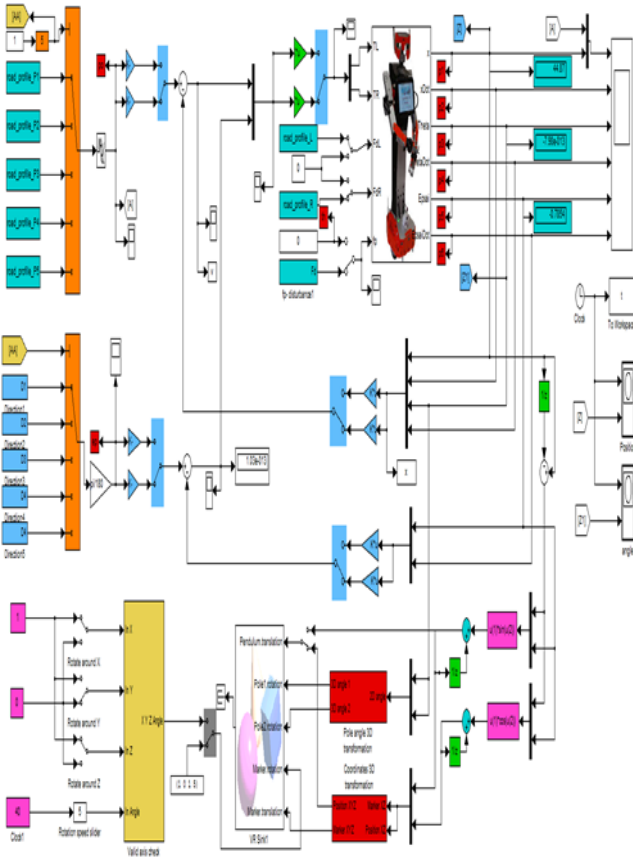


Fig. 7: The link between Simulink model and virtual world

To ensure that the controller is able to give the best performance, the system will be tested with a different set of paths as shown in Figure 8. The TWIPMR plant model will be subjected to a road_profile_L and road_profile_R disturbance acting to the left and right wheel respectively (FdL,FdR) as shown in Figure 9 and the pulse profile to the pendulum about the pitch axis (fd) as shown in Figure 10. For the purpose of controller testing, a simulation using MATLAB's Virtual Reality toolbox is achieved in next section.

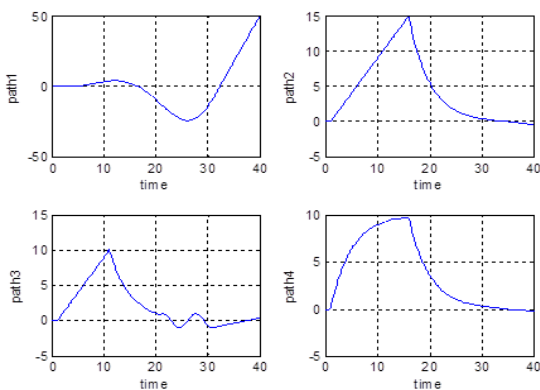


Fig 8. Profile of difference reference tracking

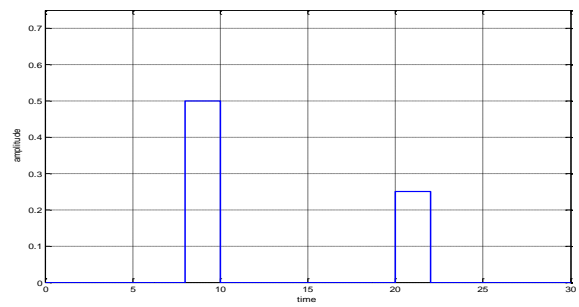


Fig 9. Profile of left and right wheel disturbance

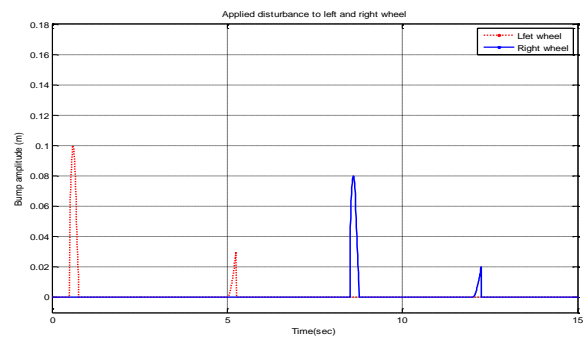


Fig 10. Profile of pulse disturbance acting at the body about the pitch axis

The simulation results in (Figs 10-12) show the performance of the considered designed control method with different reference input signals are applied. Where, an accurate tracking of the linear displacement x , rotation angle θ and rotation angle δ trajectories to these reference signals is observed.

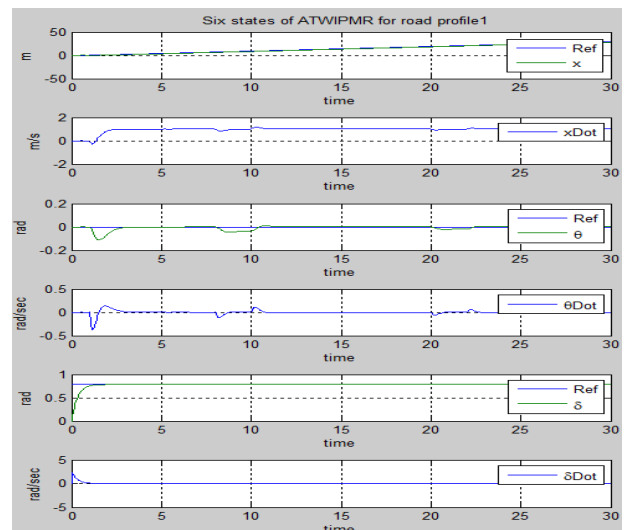


Fig 11: States of TWIPMR for road profile1

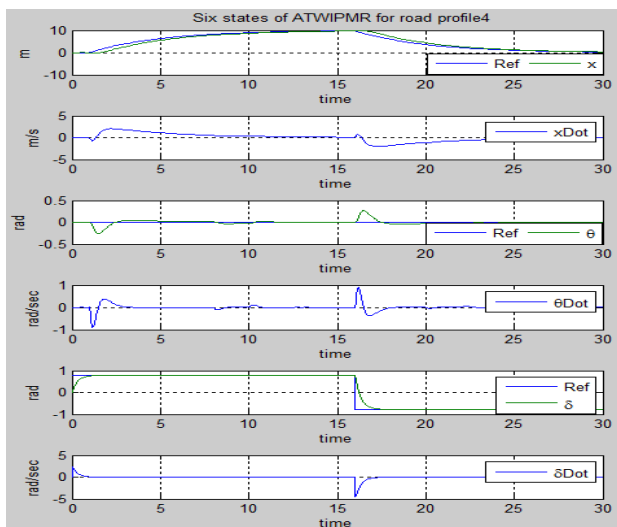


Fig 12: States of TWIPMR for road profile2

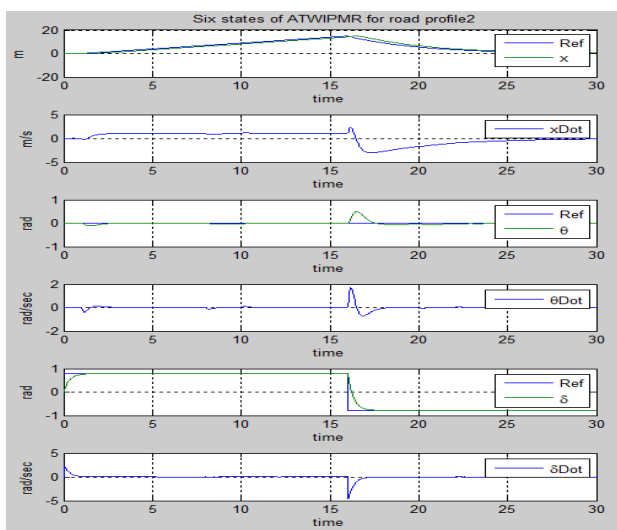


Fig. 13: States of TWIPMR for road profile3

Conclusion

In this paper, the mathematical model of the TWIPMR is presented. The balance and tracking control of the two wheeled mobile robot has been studied and analyzed. Two linear quadratic regulators with integral control and feedforward scaling factor (LQRIC and LQRFSF) have been applied as a decoupling controller to improve the system performance according to an optimal control parameters adjustment. Different input reference signals have been applied to test the effectiveness of this controller and it is demonstrated that an acceptable tracking accuracy can be achieved. It is concluded that, under the influence of these signals the decoupling controller is successful to achieve a high tracking performance in transient and steady state time. In addition, the uncertainty due to effect

of noise signal is considered to test the robustness of the control design approaches, and it is demonstrated that, the decoupling controller is robustness controller.

References

- [1] Jian Xin,Zhao Qin Guo and Tong Heng Lee “Design and Implementation of Integral Sliding-Mode Control on an Underactuated Two-Wheeled Mobile Robot,” IEEE Transactions on industrial electronics, Vol. 61, No. 7, JULY 2014.
- [2] Chenguang Yang, Zhijun Li Rongxin Cui and Bugong, “Neural Network Based Motion Control of Underactuated Wheeled Inverted Pendulum Models,” IEEE Transactions on neural Networks and learning systems, Vol. 25, No. 11, November 2014.
- [3] Hongguo Niu, Niu Wang and Nan Li, “The adaptive Control Based on BP Neural Network Identification for Two Wheeled Robot,” 12th World Congress on Intelligent control and Automation (WCICA),June 12-15, China, 2016.
- [4] Ahmad and Osman, “Real-Time Control System for a Two-Wheeled Inverted Pendulum Mobile Robot,” Advanced Knowledge Application in Practice University Technology, Malaysia, 2015.
- [5] Steven J. Witzand, “Coordinated LEGO Segways,” MSc The University of New South Wales, 2009.
- [6] A.S. Andreyev, O.A. Peregudova, “The motion control of a wheeled mobile robot”, Journal of Applied Mathematics and Mechanics,2015.
- [7] Felix Grasser, “JOE: A Mobile, Inverted Pendulum,” Laboratory of Industrial Electronics Switzerland, 2015.
- [8] Shinya Akiba,” Optimal tracking control of two-wheeled mobile robots based on model predictive control” The 11th IEEE International Workshop on Advanced Motion Control March 21-24, 2010, Nagaoka, Japan
- [9] Shagging Jiang, Fuquan Dai, Ling Li and Xueshan Gao,” Modeling and LQR Control of a Multi-DOF Two-wheeled Robot”,Proceedings of the 2014 IEEE International Conference on Robotics and Biomimetics December 5-10, 2014, Bali, Indonesia
- [10] Wei An and Yangmin Li, “Simulation and Control of a Two-wheeled Self-balancing Robot,” Proceeding of the IEEE, International Conference on Robotics and Biomimetics (ROBIO), Shenzhen, China, December 2013.